APPLICATION OF SATELLITE AVHRR TO WATER BALANCE, MIXING DYNAMICS, AND THE CHEMISTRY OF LAKE EDWARD, EAST AFRICA

JOHN T. LEHMAN

Department of Biology and Center for Great Lakes and Aquatic Sciences, University of Michigan, Ann Arbor, MI 48109-1048, USA

ABSTRACT

Surface heat balance and evaporation rates for Lake Edward were calculated as part of a model for mixed layer dynamics. Evaporation rates were combined with rainfall and fluvial income to estimate water balance. Heat and water balance were subjected to sensitivity analyses to evaluate the relative effects of variations in minimum and maximum air temperature, humidity, wind speed, cloud cover, and rainfall. Cloud cover and wind speed emerged as the most influential factors for lake temperature, evaporation, and mixing dynamics. Historical variations in ionic strength of Lake Edward surface water underscore sensitivity of the lake to climate. Major ion composition of the lake is incongruous with chemical inputs reported for streams descending from the Ruwenzoris and the highlands of southwestern Uganda. Mass balance calculations reveal that major sources of many elements are unaccounted for by present measurements, and point to the dominance of as yet unstudied stream sources entering the lake from the Virunga volcano region at the south. Based on model calculations, the chemical composition of water sources from the Virunga region is predicted a priori. Lake Edward is remarkable because despite episodic richness of biogenic Si in its sediments, diatoms are not common at present, although they are more prevalent in the south than in the north. One reason for episodic success by diatoms may be linked to changing patterns of lake mixing. Seasonal mixing dynamics of the lake were inferred from weather records and radiation flux measured from Advanced Very High Resolution Radiometer (AVHRR)

E.O. Odada and D.O. Olago (eds.),
The East African Great Lakes: Limnology, Palaeolimnology and Biodiversity, 235–260.

satellite data. SSTs inferred from AVHRR imagery were used to test one hypothesis for the diatom distribution- namely that increased water column stability in the north and a shoaling mixed layer exaggerate the loss rates by sinking and depress the supply of nutrients from below. Variations in water balance for the lake are consistent with observations of significant changes in lake water chemistry during the 20th century.

1. INTRODUCTION

The Great Lakes of East Africa are rich sources of information about climatic variations in recent times as well as over long periods of human history and prehistory (Johnson and Odada, 1996). Paleolimnology has revealed that Lake Victoria, a major source of the White Nile, was dry during the last glacial period, and began to overflow comparatively recently (Johnson *et al.*, 1996; Johnson *et al.*, 1998). The great African lakes are sensitive indicators of climate, and several of them offer long sedimentary records. One such lake is Edward, a half graben on the equator in the Western Rift at the border of Uganda and the Republic of the Congo. Despite potentially rich geological history, it is little studied and remains largely unknown in many respects.

Water balance and mass budgets for chemical constituents provide essential framework for climate studies. No such framework has previously been assembled for Lake Edward, but there are indications that the lake is dynamic and responsive to climate variations. Surveys of its water chemistry during the past 40 years have identified two-fold changes in total ionic composition (Lehman *et al.*, 1998). The lake is noteworthy for its relatively high ionic strength despite being one of the headwater sources of the White Nile. The other headwater source, Lake Victoria, is of markedly lower ionic strength. Talling and Talling (1965) remarked on its unusual ion ratios, particularly its high contents of Mg and K. They ascribed its unusual chemistry to basic volcanic source rocks in the catchment. Degens (1973) stated that Edward, and all of the lakes of the African Western Rift, were influenced by hydrothermal inputs. If hydrothermal influences are indeed pervasive, there could be anomalies in material and possibly even heat budgets for the lake.

This study assembles meteorological, hydrological, and chemical data for Lake Edward and its catchment and organizes them into a coherent model for the lake. The model is based on principles of mass and heat balance constrained by existing data. The relative influence of different climate variables on water balance and mixing conditions is assessed. The purpose of the study was to collect, review, and analyze existing data so as to identify gaps in existing knowledge, as well as to uncover potential inconsistencies in the existing data record.

2. STUDY SITE

Lake Edward (Figure 1) receives drainage from the southwestern Ruwenzoris to the north, the highlands of Rwanda and SW Uganda (Kigezi district) to the east, and the Virunga volcanoes to the south. Net inflow occurs through the Kazinga Channel from a shallow but optically deep and hypereutrophic northeastern extension, Lake George. Lake George and its surrounding catchments were studied during the 1960s as part of a Royal Society component of the International Biological Programme (IBP) (Burgis *et al.*, 1972). Lake Edward itself is anoxic below ca. 40 m to its maximum depth of ca. 120 m, but it is only weakly chemically stratified. The temperature difference between surface and deep waters of the lake is only about 1 °C maximum, with surface temperatures around 26 °C. There is thus reason to believe that the lake circulates seasonally, but no time series of observations exist to confirm the deduction. The stratigraphic record in its sediments extends for at least hundreds, and probably a few thousand, meters (Degens, 1973).

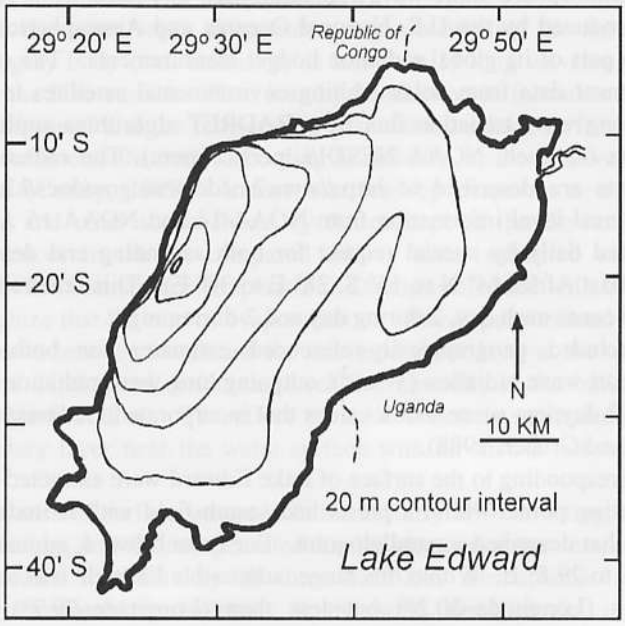

Figure 1. Lake Edward bathymetry, redrawn from original by T. Lærdal.

The sediments of Lake Edward are a rich diatom ooze, with biogenic silica varying between 5% and 50% by mass of the sediment (Johnson and Kelts, personal communication; J. Russell *et al.*, ms. in preparation). Authogenic calcite constitutes about 10% by mass on average, with marked temporal variation. Recently, the

diatom flora has been weakly developed in the lake, particularly in the north (Hecky and Kling, 1987), although Worthington (1932) mentioned a conspicuous increase in diatoms along a transect from the Kazinga Channel into northern Lake Edward in 1931. Diatoms were nearly absent from northern lake sites sampled in 1995, consistent with diminished diatom representation in surface sediments (Lehman *et al.*, 1998). Dissolved silicate is abundant at present (150 μM SRSi, Lehman *et al.*, 1998), and is not being reduced to low levels by the biogenic precipitation typical of many lakes. The enormous concentrations and variability of fossil diatoms suggest that the present condition is aberrant, but not unique because wide variation in biogenic Si is a feature of the stratigraphic record.

3. DATA SOURCES

Analysis of radiation balance components requires information about insolation, cloud cover, and surface meteorology at appropriate geographic scales. Cloud cover and top-of-atmosphere short wave radiation were extracted from radiation budget estimates produced by the U.S. National Oceanic and Atmospheric Administration (NOAA) as part of its global radiation budget measurements. The radiation budget relies on sensor data from polar orbiting environmental satellites to compute short wave and long wave radiation flux from RADRET algorithms applied to Level 1b satellite data (I. Guch, NOAA NESDIS, pers. comm.). The radiation budget flux measurements are described at http://www2.ncdc.noaa.gov/docs/klm/html/c9/sec9-3.htm. Retrieval level information from NOAA-14 and NOAA-15 AVHRR sensors were obtained daily by special request for both ascending and descending orbital paths over East Africa (4° N to 15° S, 28° E to 38° E). This remote sensing scheme provided 4 scenes each day, 2 during day and 2 during night.

Data included geographically-referenced estimates for both available and absorbed short wave radiation (W m^{-2}), outgoing long wave radiation (OLR, W m^{-2}), as well as 12 daytime scene index values that incorporate cloudiness on a four point scale (Ruff and Gruber, 1988).

Data corresponding to the surface of Lake Edward were extracted from the larger set by selecting points within a prescribed search field with latitude and longitude boundaries that described a parallelogram. For Lake Edward, admissible Longitude was 29.3° E to 29.8° E. Within this range, admissible Latitude was constrained to be greater than (Longitude–30.2°) but less than (Longitude–29.7°). Binary data received from NOAA in sequential EDGEIS file format were extracted by software written by the author in Visual Basic.

Daily maximum and minimum air temperature, wind speed, barometric pressure, and dew point were extracted from Global Summary of Day climate observations from 1994 to 1998 for Kasese, Uganda (Stn 636740: 0° 11' N, 30° 6' E, elevation 961 m) archived by the National Climate Data Center (NCDC). Data may be accessed by way of http://www.ncdc.noaa.gov/cgi-bin/res40.pl?page=gsod.html. Mean values for each month were calculated for the reference period and the monthly means were used in model calculations.

Precipitation estimates for the geographic region around Lake Edward were obtained from NCDC archives in the Global Historical Climate Network version 2 (URL: http://www.ncdc.noaa.gov/cgi-bin/res40.pl?page=ghcn.html). Mean monthly precipitation estimates were obtained for ten stations ranging from 1.3° S to 0.8° N, and from 29.4° to 30.6° E, at elevations ranging from 920 to 2300 m.

3.1 Conceptual Overview

Changes in heat content and seasonal mixing depth of lakes and surface ocean waters are consequences of heat and momentum fluxes (Price, 1981; Monismith, 1985; Spigel *et al.,* 1986; Spigel, 1980; Spigel and Imberger, 1980; Imberger and Patterson, 1990). Heat gained from irradiance is lost to the atmosphere over time. The heat loss mechanisms are by long wave radiation, conduction, and evaporation; outflow losses of heat must be considered in some cases. Net heat loss by long wave radiation depends on the temperature difference between surface water and the sky as well as humidity and cloud cover (Keijman, 1974).

Variation in the water vapor or greenhouse gas content of the atmosphere can change the net gray body (i.e., emissivity is less than 1) long wavelength radiative heat flux from the lake surface. Heat loss by conduction is formulated as a linear function of wind speed and the temperature gradient from lake surface to air, with bulk transfer coefficients that vary according to stability, or the relative temperature of lake and air (Croley, 1989). Latent heat loss by evaporation is linked with conduction loss and other scalar fluxes by the concept of the Bowen ratio, using humidity differences in the air compared with a water saturated atmosphere at equilibrium with the lake surface temperature. Dalton is credited with being the first person to recognize that the rate of evaporation of water is proportional to the vapor pressure difference between the air and the saturated vapor layer at the water surface. Either decreased wind speed or increased relative humidity in the bulk atmosphere will decrease this heat flux. The effect of wind action is to replace the vapor-saturated boundary layer near the water surface with air that is not saturated with water vapor.

The heat balance of surface waters is fundamentally self-correcting; a temporary decrease in heat loss will be compensated for by elevated water temperature, with resultantly increased heat flux by all three heat loss mechanisms. When each mechanism is considered in isolation, if the wind slows down, or if the air temperature rises, or if the humidity increases, or if the sun shines more brightly, in each case the surface warms.

4.0 HYDROLOGY AND BALANCES FOR HEAT, WATER, AND CHEMICAL CONSTITUENTS

4.1 Heat Balance

Lake heat content is considered to be the result of a balance among short wave and long wave radiative fluxes, evaporation, and heat conduction. The energy balance model is

$$\Delta \text{ Lake Heat} = SW_{net} + LW_{net} - LH - SH \quad (1)$$

where SW is short wave radiation, LW is long wave radiation, LH is latent heat loss by evaporation and SH is sensible heat loss by free and forced convection. The scaling constants in equations were chosen to permit calculation of heat flux in cal cm^{-2} d^{-1}. Net short wave radiation received into the lake water is calculated as insolation measured at the ground (SW_0) reduced by lake albedo (α):

$$SW_{net} = (1 - \alpha)\, SW_0 \quad (2)$$

where $\alpha = 0.07$ (Yin and Nicholson, 1998). Incident SW_0 is calculated from satellite-derived measurements of available SW at the top of the atmosphere ($SW_{available}$) by using a correction for cloud effect (Yin and Nicholson, 1998):

$$SW_0 = SW_{available}\,(0.803 - 0.34\,C - 0.458\,C^2) \quad (3)$$

where C is the fraction of sky occluded by clouds. The NOAA radiation budget calculations generated mean daily $SW_{available}$.

Net heat loss by long wave radiation is estimated as gray body radiation upward from the lake surface combined with counter-radiation of LW radiation downward from the atmosphere, using the approach introduced by Keijman (1974) and subsequently adopted for modeling evaporation in the St. Lawrence Great Lakes (Croley, 1989):

$$LW_{net} = \sigma\, T_{Air}^4\,(0.53 + 0.065\, e_{Air}^{0.5})(p + (1 - p)(1 - C)) - \varepsilon\, \sigma\, T_L^4 \quad (4)$$

where ε is emissivity (= 0.97 Strub and Powell, 1987), σ is the Stefan-Boltzmann constant, T_L and T_{Air} are lake surface and air temperature (K), e_{Air} is atmosphere vapor pressure (mb), and p is a dimensionless parameter.

Heat losses by evaporation and conduction are computed from heat and vapor pressure gradients using bulk coefficients estimated for the turbulent atmospheric boundary layer over the lake. Two different methods were used to estimate the transfer coefficients. In one case (Model 1), bulk transfer coefficients were calculated by the iterative algorithm published by Croley (1989, his eqs. 1 to 10).

This method involved application of Monin and Obukhov's similarity hypothesis to wind speed and air temperature:

$$U = U^* / \kappa \, [\ln(Z/Z_L) - S_1] \quad (5)$$

$$T - T_L = T^*[\ln(Z/Z_L) - S_2] \quad (6)$$

Where U is mean wind speed at reference height Z above the surface, U^* is friction velocity, κ is von Karman's constant, Z_L is roughness length, T is potential temperature at reference height, T_L is potential temperature at Z_L, and T^* is the scaling temperature defined as

$$T^* = Q_H /(r \, C_P \, \kappa \, U^*) \quad (7)$$

where C_P is the specific heat of air at constant pressure, Q_H is the turbulent heat flux to the surface, and r is air density.

The second approach (Model 2) was to approximate evaporation, or latent heat flux, by the bulk formula proposed by Maidment (1993):

$$\text{Evap (cm d}^{-1}) = 0.02909(\text{Lake Area, m}^2)^{-0.05} (e_L - e_{Air}) \quad (8)$$

Saturation vapor pressure at the temperature of the lake surface was defined (Maidment, 1993) as

$$e_L = 6.11 \exp(17.3 \, T_L/(T_L+237.3)) \quad (9)$$

Heat balance is thus a function of SW_0, T_L, T_{Air}, e_{Air}, C, and wind speed. Table 1 summarizes the key parameters and their definitions.

4.2 Theory of the Surface Mixed Layer

Modern synthesis of theory about the surface mixed layer is typically credited to Niiler and Kraus (1977). They drew on earlier studies to summarize how wind stress and buoyancy forces erode an existing thermocline. They are credited with solving the problem of the seasonal thermocline. Subsequent studies have extended the theory of the seasonal thermocline to the diurnal mixed layer.

Solar radiation that penetrates a lake surface is ultimately absorbed and converted to heat. Because the specific volume of water, and alternatively its density, are nonlinear functions of temperature, the absorption of heat causes buoyancy changes. Light attenuates differentially according to wavelength. The solar irradiance at longer wavelengths (IR) is absorbed within the top 2 meters or less by water itself. Light at shorter wavelengths, particularly 400-700 nm (PAR: photosynthetically

active radiation), which is the photosynthetic and visible part of the spectrum, penetrates more deeply. Its attenuation rate varies strongly with dissolved and particulate matter in the water. In particular, PAR penetration varies inversely with algal biomass.

Heat loss occurs at the lake surface. The result is a cooled surface film. At temperatures greater than 4°C, the cooling generates convection by water that becomes denser than the water just below. The kinetic energy of resulting convection cells adds to kinetic energy produced by wind stress. The two sources of kinetic energy provide the turbulence velocity shears that work against any existing stable density gradient at the base of the turbulent mixed layer. During daytime, however, light absorption is a buoyancy generating mechanism that acts as a sink for this kinetic energy.

Table 1. Parameter definitions for heat balance model applied to Lake Edward.

Parameter	Definition	Formula	Units
T_L	lake surface temperature		°C
T_A	air temperature		°C
T_{DP}	dewpoint temperature		°C
U	mean wind speed at 2 m		m s^{-1}
C	Fraction cloud cover		none
P_{STA}	Atmospheric pressure at lake		mb
σ	Stefan-Boltzmann constant	8.26×10^{-11}	cal cm^{-2} min^{-1}
ε	water emissivity	0.97	none
α	lake albedo	0.07	none
p	effect of clouds on LW_{down}	0.6	none
C_P	specific heat of dry air	0.2403	cal g^{-1} K^{-1}
$SW_{available}$	SW at top of atmosphere		cal cm^{-2} d^{-1}
A	lake surface area	2325×10^6	m^2
SW_0	Incident short wave radiation	$SW_{available}$ (0.803 –0.34 C –0.458 C^2)	cal cm^{-2} d^{-1}
e_A	air vapor pressure	6.11 exp(17.3 T_{DP}/(T_{DP}+237.3))	mb
e_L	saturation vapor pressure at	6.11 exp(17.3 T_L/(T_L+237.3))	mb
LVT	Latent heat of vaporization at	597.3 – 0.564 T_L	cal g^{-1}
B	Bowen ratio	C_P(T_L-T_A)/LVT(e_L– e_A)	none
EVAP	Evaporation	0.02909 U $A^{-0.05}$(e_L– e_A)	cm d^{-1}
LH	Latent heat flux	LVT × EVAP	cal cm^{-2} d^{-1}
SH	sensible heat flux	LH × B	cal cm^{-2} d^{-1}
LW_{net}	net long wave radiation to	$\sigma(T_A+273.15)^4(0.53+0.065e_{Air}^{0.}$	cal cm^{-2} d^{-1}
SW_{net}	net shortwave radiation to	(1-α) SW_0	cal cm^{-2} d^{-1}
Balance		SWnet + LWnet –LH – SH	cal cm^{-2} d^{-1}

Light attenuation is strongly nonlinear, such that more light is absorbed at the top half of any water layer than in the bottom half of the same layer. The result is

continual production of positive buoyancy while the sun is shining. Turbulence kinetic energy is either partially or completely expended by working to mix the water in opposition to these buoyancy forces. As a result, during full sunlight hours the diurnal mixed layer shoals and mixing is contained much closer to the surface than during the night. Daytime mixed layer thickness can be predicted from irradiance, light attenuation, and the kinetic energy from wind and surface cooling.

Throughout the night, the mixed layer deepens as large convection cells, forced by the wind if it is present, entrain cool water at the base of the layer. The rate of layer deepening is set by the "generalized entrainment law" (Sherman *et al.*, 1978), which considers available kinetic energy, convection cell size, and the potential energy represented by stable density stratification that opposes the entrainment forces. It takes energy to pull cooler, dense water from the bottom of the mixed layer and lift it upward against gravity. As a result of the overnight process driven by surface cooling, the maximum extent of vertical mixing is typically reached at or around dawn.

4.3 Diffusion Processes Below the Mixed Layer

Mixing processes below the turbulent mixed layer were modeled for this study as eddy diffusion, using a constant diffusion coefficient of 0.02 $cm^2 s^{-1}$. Imberger and Patterson (1990) cite this value as a lower limit of diffusion rates below the mixed layer, and it is probably most appropriate to the region of high gradient diffusive fluxes immediately below the surface layer. This coefficient probably underestimates eddy diffusion in the bulk of the hypolimnion, but is inconsequential to mixed layer dynamics and surface heat flux.

4.4 Sensitivity Analysis

Sensitivity analysis for the heat balance model was conducted by specifying a "standard" climate condition equal to empirical mean monthly conditions for air temperature, dew point, insolation, station barometric pressure, fraction cloud cover and wind speed. Day-of-month conditions were obtained by linear interpolation of the monthly means, assuming that the means represented conditions at mid-month. Simulations over an entire year were conducted with a horizontally averaged mixed-layer model using a time step of one hour.

Air temperature was simulated from the daily maximum and minimum records by assuming that minimum temperature occurred at sunrise, and that maximum temperature occurred midway between noon and sunset. Air temperatures at other times were obtained by linear interpolation. The initial condition for lake temperature was specified by running the model for one year under the "standard" climate scenario starting with an isothermal water column at 25.5 °C. The final

calculated temperature distribution at the end of the year was stipulated as the initial state for all further simulations.

A reference, or Base simulation was conducted by running the model for one year under the standard mean climate conditions as specified in Table 2. Then, each climate variable was independently both increased and decreased by finite steps, and the response variables were recalculated by annual simulations for each perturbation. The magnitudes of the step perturbations were in proportion to the statistical variability of empirical climate data. Specifically, the standard deviation of each climate variable in the Kasese data set was calculated by month for data pooled across years. For each month and each climate variable, a day to day standard deviation ($SD_{i,m}$) was computed where i indicates the climate variable and m represents month. An index for variability of monthly means was defined as double the expected 30-day random sample standard error from the pooled data:

$$Dev = 2 \times SD_{i,m} / \sqrt{30} \qquad (10)$$

This index, when either added or subtracted from the mean value, was taken to approximate a 95% confidence interval for year-to-year variation in mean climate values for any given month.

Table 2. Mean values by month for climate variables, and magnitudes of perturbations (Dev, from Eq. 10) used for sensitivity analysis.

	Air T_{MAX} °C		Air T_{MIN} °C		T_{DP} °C		U m s^{-1}		Cloud fraction	
	Mean	Dev	Mean	Dev	Mean	Dev	Mean	Dev	Mean	Dev
Jan	29.9	0.77	18.2	1.01	19.01	0.51	2.41	0.29	0.413	0.105
Feb	29.5	0.91	17.8	0.70	17.81	0.72	2.14	0.29	0.305	0.081
Mar	28.6	1.28	18.6	0.68	19.02	0.36	2.48	0.44	0.481	0.100
Apr	28.7	0.96	19.2	0.95	19.73	0.47	2.14	0.25	0.333	0.082
May	29.1	0.93	18.1	0.78	19.66	0.40	2.00	0.63	0.257	0.078
Jun	28.3	0.90	18.0	0.75	19.00	0.35	1.65	0.48	0.292	0.079
Jul	28.0	1.04	19.1	1.55	18.15	0.54	1.66	0.24	0.318	0.084
Aug	29.8	0.78	17.6	0.88	17.44	0.54	2.22	0.60	0.494	0.106
Sep	29.8	0.97	17.9	0.80	18.72	0.32	2.68	0.62	0.353	0.093
Oct	28.9	0.79	17.8	0.69	19.13	0.28	2.67	0.40	0.370	0.099
Nov	28.1	0.82	18.6	0.76	19.40	0.28	2.33	0.31	0.517	0.100
Dec	28.6	0.73	17.8	0.88	19.15	0.38	2.33	0.39	0.420	0.093

The differential effects of each independent climate factor (e.g., air temperature, dew point temperature, wind speed, or fractional cloud cover) on each response variable (e.g., lake surface temperature, mixing depth, evaporation rate) were then compared against the standard reference conditions. The variations defined in Eq. 10 are tabulated by month for each independent climate variable in Table 2. Top of atmosphere short wave radiation and barometric

pressure were tabulated by month as mean values only in Table 3; insufficient data existed to identify the magnitudes of interannual variation in these two latter variables.

Table 3. Monthly means for top-of-atmosphere short wave radiation and station barometric pressure.

	$SW_{available}$	P_{STA}
	$W\ m^{-2}$	mb
Jan	421.8	903.6
Feb	435.2	903.5
Mar	438.6	903.4
Apr	423.6	904.7
May	400.6	905.7
Jun	386.1	904.9
Jul	391.2	905.6
Aug	411.7	905.1
Sep	428.8	905.1
Oct	432.5	904.3
Nov	422.6	903.8
Dec	415.0	904.3

4.5 Hydrologic Model for Lake Edward

Hydrologic characteristics of Lake Edward and its catchment are assembled from data provided by Viner and Smith (1973), Bugenyi (1982), Hecky and Kling (1987), ILEC (2000), and Lærdal *et al.* (2001). Different sources are not in agreement about such fundamental points as lake mean depth (and volume) or catchment area. The modern bathymetry measured by Lærdal *et al.* (2001) was adopted and values are reported in Table 4. Drainage basin boundaries for Africa were taken from HYDRO1k, a hydrologically correct 1-km resolution version of the GTOPO30 global 30 arc-second Digital Elevation Model produced by the USGS EROS Data Center (Figure 2). The data and derivations are described at http://edcdaac.usgs.gov/gtopo30/hydro/readme.html. Water balance for Lake Edward was calculated as

Outflow = Input from catchment + direct precipitation – evaporation (11)

Direct precipitation on the lake surface was taken to be the mean of the annual average precipitation at 10 stations around Lake Edward (1214 mm yr^{-1}). Six of the stations are located inside the catchment boundary, and the others are close by (Figure 2). The data represented 470 station-years of record ranging from 19 to 87

years per station. Precipitation did not vary significantly with elevation among these stations (Figure 3). Moreover, annual precipitation was not well correlated among the 10 stations. In 44 pairwise correlations the mean correlation was 0.25 (range = -0.23 to 0.76), and only 8 station pairs exhibited correlation greater than 0.5. The estimated precipitation reported by Viner and Smith (1973) for Lake George is 30% lower than the average value of 1214 mm yr^{-1} found here, but it is within the range of variation of the data among stations.

Figure 2. HYDRO1k drainage basin boundaries with Pfafstetter Level 4 codes, stream drainage (DCW, 1993), and GHCN version 2 climate stations.

Water input from the catchment was estimated by the method of Viner and Smith (1973). Total runoff was estimated from measurements of runoff yield by the Nyamuganasani River, which drains from the Ruwenzoris into northern Lake Edward. From measured discharge and river catchment area, Viner and Smith (1973) report 0.518 m yr^{-1} in surface runoff per m^2 of land surface. Thus, for the terrestrial catchment of Lake Edward (20374 km^2 exclusive of lake surface area), the expected mean annual water income by direct proportions is 1.06×10^{10} m^3. Because the relationship between mean precipitation and mean fluvial runoff is not known for Lake Edward catchments, the runoff yield may contain systematic bias when applied to the entire catchment area and to long term temporal averages. Hence, sensitivity analyses were used to infer the potential importance of these different assumptions.

Table 4. Morphometry and hydrology of Lake Edward.

Surface Elevation	912 m
Lake area	2325 km^2
mean depth	33 m
Lake Volume	7.67×10^{10} m^3
Catchment Area (less lake)	20374 km^2
Kazinga Channel discharge	1.70×10^9 m^3 yr^{-1}
Nyamugansani River discharge	0.26×10^9 m^3 yr^{-1}
direct rainfall	2.82×10^9 m^3 yr^{-1}
Other fluvial income	8.59×10^9 m^3 yr^{-1}
Outflow at Semliki River	1.08×10^{10} m^3 yr^{-1}
Evaporation	2.59×10^9 m^3 yr^{-1}
Lake Volume/Outflow	7 yr
Lake Volume/Evaporation	30 yr
Theoretical concentration factor for conservative solutes	1.2

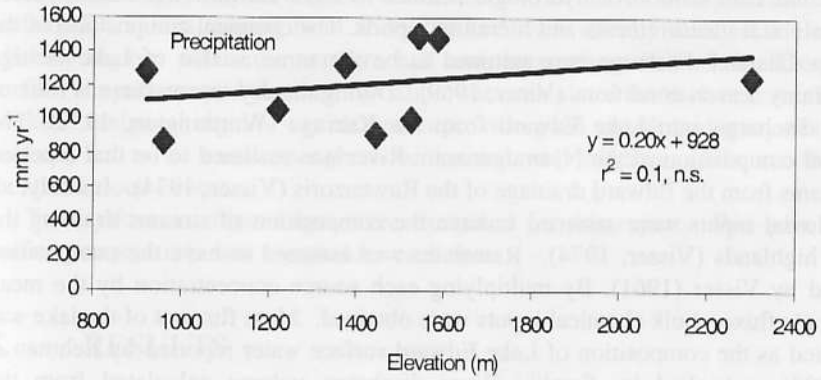

Figure 3. Mean annual precipitation versus elevation for 10 climate stations near Lake Edward.

Historical measurements were used for discharge of the Nyamuganasani River and Kazinga Channel into northern Lake Edward (Viner and Smith, 1973). Residual hydrologic income was assumed to derive from streams visible in Figure 2 including (1) the Lubilia River forming the international boundary at the north of the lake and also draining from the Ruwenzoris, (2) the Ishasha forming the international boundary at the south of the lake, and together with the Ntungwe, Mehuera, Ruampuno and Niamweru draining from the Kigezi and Ankole highlands of SW Uganda into the southeastern shore of the lake, (3) the Ruchuru and other unnamed streams draining the rift north of the Virunga volcanoes, and (4) miscellaneous unnamed mountain torrents which cascade from the Congo escarpment at the west. The HYDRO1k data set identifies two major sub-catchments for Lake Edward. Catchment 2967 includes drainage from the Ruwenzoris, Lake George, and the Uganda highlands. Catchment 2966 is dominated by drainage from the Virunga district but also includes the Congo escarpment.

Sensitivity analysis was conducted to evaluate the potential impact of regional variations in rainfall. Annual rainfall at ten stations around Lake Edward (GHCN version 2, National Climate Data Center archives: http://www.ncdc.noaa.gov/cgi-bin/res40.pl?page=ghcn.html) exhibits a mean CV (Coefficient of Variation = ratio of Standard Deviation to Mean) of 0.188 (SD = 0.056). Approximation of a 95% probability range for annual regional precipitation was assumed to be the mean (1214 mm) plus or minus double this CV multiplied by the mean. The same CV (i.e., 0.188) was assumed representative of total surface runoff.

4.6 Chemical Balance

The ion composition of hydrologic sources to Lake Edward was reconstructed from historical measurements and literature reports. The chemical composition of the Kazinga Channel discharge was assumed to be the same as that of Lake George during rainy season conditions (Viner, 1969). During the dry season there is little or no net discharge into Lake Edward from the Kazinga (Worthington, 1932). The chemical composition of the Nyamuganasani River was assumed to be that reported for streams from the Edward drainage of the Ruwenzoris (Visser, 1974). Initially, all other fluvial inputs were assumed to have the composition of streams draining the Kigezi highlands (Visser, 1974). Rainwater was assumed to have the composition reported by Visser (1961). By multiplying each source concentration by the mean hydrologic fluxes, bulk chemical inputs were obtained. Mass flux out of the lake was calculated as the composition of Lake Edward surface water reported by Lehman *et al.* (1998) multiplied by Semliki River discharge volume calculated from the hydrologic model.

Sediments of Lake Edward consist of rich siliceous ooze with about 40% SiO_2 by weight on average, 1.2% sulfur, and at least 15% calcite; most of the carbonates are $CaCO_3$, but about 12% are $MgCO_3$ (J. Russell *et al.*, ms. in preparation). Sediment accumulation rates are roughly 0.1 cm yr^{-1}. At sediment density of 2.5 g cm^{-3}, and porosity of 0.9, the mineral content and sedimentation rates indicate about 0.33 mol

$CaCO_3$, 0.05 mol $MgCO_3$, 0.09 mol S, and 1.7 mol SiO_2 m^{-2} yr^{-1} accumulate in the sediments. Removal rates by burial must be included in mass balance calculations.

4.7 Remote Sensing of Lake Edward Surface Temperature

Surface temperatures of Lake Edward were calculated from archival AVHRR (Advanced Very High Resolution Radiometer) data sets maintained by NOAA's Satellite Active Archive. The on-line archive available at www.saa.noaa.gov was searched for relatively cloud-free images of Lake Edward during 1995, 1996, and 1999. Suitable scenes at Local Area Coverage (LAC) resolution, nominally 1.1 km at satellite nadir, were downloaded in 10-bit Level 1B format. Spectral channel data were extracted from the packed binary files by XV-HRPT Data Acquisition software, version 4.3. The software was purchased from Dr. A. Mazurov, Space Research Institute RAS, Moscow (http://smis.iki.rssi.ru). Surface lake temperature in degrees C was calculated by multichannel split (MCSST split) algorithms for day or night images using the brightness temperatures (°K) recorded in AVHRR channels 4 and 5, and the calculated satellite zenith angles. Equations and calibration coefficients for NOAA-12 and NOAA-14 polar orbiting environmental satellites (POES) were used directly from values published by NOAA at http://psbsgi1.nesdis.noaa.gov:8080/EBB/ml/nicsst.html. It was not possible to calibrate the equations specifically for Lake Edward owing to the absence of contemporaneous lake surface temperature measurements.

The calculated SSTs were encoded as 8-bit scalar representations of their numerical values, and were projected and visualized as gray-scale images at 1-km resolution on a rectangular coordinate system by XV-HRPT software, using the latitude and longitude geo-reference data embedded in the AVHRR scan lines. Then, rectangular regions ranging from 36 to 289 km^2 were visually selected in cloud free offshore regions within the northern half and the southern half of the lake. Mean surface temperature and standard deviation were calculated for each region. The size of these analytical regions was chosen to provide good sampling density at the lake surface, but to be small enough to be located well offshore while avoiding any localized cloud cover.

Twenty-four satellite images were examined for this report. One pair of lake surface temperatures was sampled for each date.

5. RESULTS

5.1 Heat Balance Model and Sensitivity Analysis

Summary results are reported in Table 5 for the two alternative models used to calculate evaporation rates. Tables 6 and 7 report responses achieved from perturbations of the reference values during sensitivity analyses. Total mixing

duration reports the total number of days during the year when the lake is calculated to mix to its full depth.

Table 5. Model results for reference (mean) climate conditions listed in Tables 2 and 3. Results are for two alternative models of evaporation described in the text.

Response Variable	Model 1	Model 2
EVAP mm yr^{-1}	1038	1113
T_L annual mean	27.93	27.04
T_L maximum for year	29.37	28.65
T_L minimum for year	26.92	26.00
Total mixing duration, days	167	106

Sensitivity calculations treated climate variables as independent and uncorrelated. Assumption of independence is supported by climate data from Kasese, as there are no correlations among daily maximum or minimum air temperature, dew point temperature, mean wind speed, and precipitation that exceed 0.36 in pair-wise comparisons. Sensitivity calculations reveal that cloud cover and wind speed are by far the most influential climate factors, within the limits of observed natural variation. Magnitudes of perturbations used in the analyses were reported in Table 2.

Table 6. Results of sensitivity analysis for Lake Edward heat balance with evaporation Model 1.

Independent Variable	Perturbation	Δ EVAP (mm d^{-1})	ΔT_L (°C) mean	ΔT_L (°C) max	ΔT_L (°C) min	Δ mixing period (d)
T_{MAX}	Increase	-3	+0.22	+0.26	+0.14	-32
	Decrease	-1	-0.21	-0.16	-0.23	+18
T_{MIN}	Increase	+15	+0.15	+0.17	+0.11	-7
	Decrease	-14	-0.14	-0.15	-0.15	+22
T_{DP}	Increase	-7	+0.15	+0.17	+0.10	-20
	Decrease	+7	-0.14	-0.10	-0.12	+21
U	Increase	+77	-0.60	-1.03	-0.58	+30
	Decrease	-93	0.74	+1.48	+0.25	-71
Cloud	Increase	-284	-1.35	-1.26	-1.69	+31
Fraction	Decrease	+239	+1.08	+1.18	+0.17	-56

Table 7. Results of sensitivity analysis for Lake Edward heat balance using evaporation Model 2.

Independent Variable	perturbation	Δ EVAP (mm d^{-1})	ΔT_L (°C) mean	ΔT_L (°C) max	ΔT_L (°C) min	Δ mixing period (d)
T_{MAX}	Increase	+22	+0.13	+0.19	+0.14	-2
	Decrease	-22	-0.13	-0.18	-0.14	+3
T_{MIN}	Increase	+20	+0.12	+0.14	+0.13	-6
	Decrease	-21	-0.13	-0.14	-0.13	+19
T_{DP}	Increase	-15	0.19	+0.24	+0.17	-2
	Decrease	+14	-0.19	-0.20	-0.18	+4
U	Increase	+91	-0.61	-1.04	-0.56	+83
	Decrease	-106	+0.78	+1.57	+0.21	-25
Cloud	Increase	-229	-1.41	-1.39	-1.83	+90
Fraction	Decrease	+222	+1.27	+1.30	+0.36	-33

5.2 Water Balance

Semliki River discharge from Lake Edward was calculated by difference from total surface runoff, direct precipitation, and evaporation. Historical direct measurements from the IBP period exist for hydrologic inputs from the Kazinga Channel, the Nyamuganasani River, and rainfall. Monthly precipitation and pan evaporation at Mbarara from 1969 to 1974 (Hydromet, 1991) exhibit no significant correlation between the two variables ($R = -0.162$, $n = 68$). Consequently, the effects of variability in precipitation was simulated independently from variations in evaporation rate.

The estimated Semliki outflow in Table 4 is about double the 5×10^9 m^3 yr^{-1} calculated by Hurst (1927), about triple the equivalent annualized flow rate measured by Worthington (1932) during dry season conditions in June 1931 (ca. 3.3×10^9 m^3 yr^{-1}), and about 5 times the mean discharge reported by Talbot *et al.* (2000). Hurst had estimated the catchment area at 12000 km^2, much smaller than the modern DEM now indicates (Figure 2).

Mean annual outflow is about 80% of total water income to Lake Edward, leading to a theoretical concentration factor of 1.2 for conservative solutes. Surface runoff was scaled proportionally to variations in regional precipitation for sensitivity analysis. The range of variation in theoretical concentration factor for the ranges examined (approximating a 95% Confidence Interval) was 1.1 to 1.6 (Table 8). Results are shown in Table 8 for evaporative flux Model 1; results from Model 2 were essentially the same. Again, cloud cover emerged as the most influential climate variable other than variation in precipitation itself. These results imply variations in ionic strength of about 40%, which is less than has actually been observed for Lake Edward surface water over several decades (Lehman *et al.*, 1998). Ionic strength has varied by nearly a factor of two. Evaporation can produce only a few percent increase in salt concentrations of the lake during a single dry season. In

addition to climate-induced variation, the cause of different salt concentrations measured in Lake Edward over the years may have to be sought in seasonal variations of the fluvial inputs to the lake.

Table 8. Theoretical concentration factors from sensitivity analysis. Results for Model 1; minimum and maximum values in bold print.

Independent Variable	Climate perturbation	Concentration factor for specified rainfall perturbation		
		reference (mean)	rainfall increase	rainfall decrease
Reference	None	1.22	1.16	1.45
T_{DP}	Increase	1.22	1.16	1.44
	Decrease	1.22	1.17	1.46
T_{MAX}	Increase	1.22	1.17	1.46
	Decrease	1.22	1.16	1.44
T_{MIN}	Increase	1.22	1.17	1.46
	Decrease	1.22	1.16	1.44
U	Increase	1.24	1.18	1.50
	Decrease	1.20	1.15	1.39
Cloud	Increase	1.15	**1.13**	1.33
Fraction	Decrease	1.29	1.20	**1.59**

5.3 Chemical Constituents and Mass Balance

Historical measurements of water chemistry in rain, Lake George, Lake Edward, Ruwenzori drainage, and streams of the Kigezi highlands (Visser, 1961; Talling and Talling, 1965; Viner, 1969) are combined in Table 9 to estimate the major element balance for the lake. The relatively conservative solutes Na, K, and Cl are far more concentrated in Lake Edward than the theoretical expectation for a conservative solute (Table 4), based on existing river and rain chemistry.

Hydrology and the bulk chemistry summarized in Table 9 underscore a geochemical anomaly about Lake Edward. The lake is far out of chemical mass balance based on existing measurements. Table 10 reports mass balance of major constituents computed from Tables 4 and 9. Massive sources are required for Na, K, Mg and bicarbonate to balance the mass budgets. There are not enough inputs of Ca, SO_4 and SiO_2 to account for measured sedimentation rates. Instead, there must be additional weathering sources of Ca, Si, as well as bicarbonate and other cations to close the water column and sediment budgets. The required ion composition and stoichiometry of the weathering product suggests an alkaline rock source material dominated by soluble carbonate salts. Absence of strong salt gradients in the lake argues against the likelihood that the salts are injected from groundwater sources.

Table 9. Mean (or rainy season) chemical composition (μM) of the main hydrologic sources to Lake Edward. "Mean Input" reports concentrations weighted by magnitudes of hydrologic fluxes in Table 4. For this calculation, all unmeasured inputs are assumed to have the chemistry measured for the Kigezi district.

Component	Ruwenzori	Kigezi	L. George	Rain	Mean Input	L. Edward	Conc factor
Na	534	478	890	74	410	3750	8.7
K	63	81	114	43	72	1620	21.7
Ca	389	215	361	1	166	310	1.7
Mg	206	216	300	0	141	1630	9.9
Cl	132	232	215	25	130	580	3.6
SO_4	208	204	188	19	117	250	1.7
HCO_3	1287	775	1250	0	577	7870	12.3
SiO_2	273	270	366	0	175	150	0.7

Kilham and Hecky (1973) classed Lake Edward with other "sodium-potassium-magnesium-bicarbonate" waters, including Lakes Kivu and Tanganyika, and considered their common chemistry to be influenced by the volcanic rocks of the Virunga district. Talling and Talling (1965) as well as Kilham and Hecky (1973) alluded to the likely importance of the basic volcanic rocks in this region to the ion balance of Lake Edward. Virtually no direct measurements are available for the water chemistry of rivers draining the Virunga mountains into Lake Edward. Hurst (1927) measured the titration alkalinity of the Ruchuru River, which drains into the south of Lake Edward from the Virunga district. He reported its alkalinity as equivalent to 17.2 mEq. Hurst remarked (p. 23) that [the Ruchuru] "is the largest stream entering the lake in the dry season and probably the most important feeder of the lake." He estimated its dry season discharge at its mouth during August 1926 at 40 $m^3 s^{-1}$, with estimated rainy season flood discharge of 130 $m^3 s^{-1}$. A median value of 85 $m^3 s^{-1}$ for average discharge amounts to 2.7×10^9 $m^3 y^{-1}$, or 31% of all the "other fluvial income" identified in Table 4.

Hurst's measurement of alkalinity permits alternative estimation of the missing river sources by inverse methods. It would take 54% of the water income from "other fluvial" sources (Table 4) to balance the alkalinity budget of the lake at a mean annual supply concentration of 17.2 mEq. The requisite flow is greater than the estimated median discharge of the Ruchuru; it represents the composite discharge from the Virunga district. In point of fact, the sub-catchment south of Lake Edward (Figure 2) represents 6000 km^2, or 55% of the residual area remaining after drainage from the Ruwenzoris and Lake George/Kazinga Channel are subtracted from the total catchment area. The model result is thus completely feasible.

River discharge with the mean annual composition identified in the rightmost column of Table 10 would close the bulk geochemical budgets for Lake Edward. This model-generated composition is reminiscent of the mixolimnion chemistry of Lake Kivu, a lake that is influenced by drainage from the Virunga district. The real chemistry of the Ruchuru River and others that flow across the broad southern plain

into Lake Edward is essentially unknown and unmeasured (Kilham, 1984). The figures presented in Table 10 thus constitute an explicit, model-based, *a priori* and quantitative hypothesis about the geochemistry of hydrologic sources to Lake Edward. They help explain the decrease in cations and carbonate from southwest to northeast in the lake that is evident in chemical analyses published by Worthington (1932, his table 3). Seasonal variations in these rather high predicted annual mean concentrations may also help to explain the two-fold range in the ionic strength of Lake Edward that has been recorded by different investigators.

Table 10. Mass balance anomalies for major chemical constituents in Lake Edward, and inverse model prediction of water chemistry for rivers entering from the Virunga district.

	Input-Outflow anomaly mol m^{-2} yr^{-1}	sediment accumulation mol m^{-2} yr^{-1}	Total required sources mol m^{-2} yr^{-1}	Hypothetical composition of missing inputs mM
Na	-14.83		14.83	7.9
K	-7.08		7.08	3.6
Ca	-0.33	0.33	0.66	0.6
Mg	-6.52	0.05	6.58	3.5
Cl	-1.63		1.63	1.0
SO_4	-0.22	0.09	0.32	0.4
HCO_3	-32.59	0.38	32.98	17.2
SiO_2	0.60	1.67	1.07	0.8

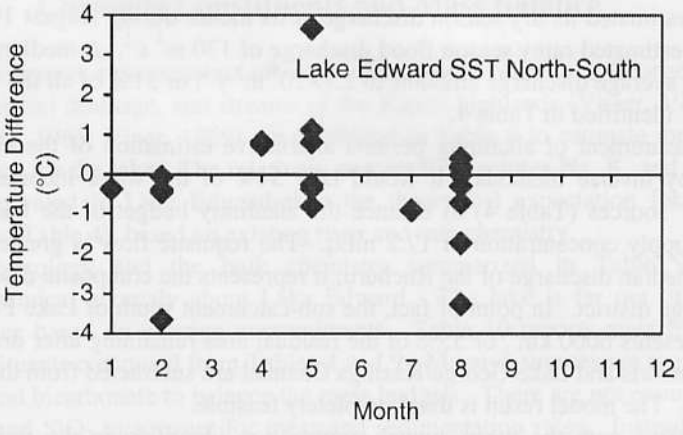

Figure 4. Temperature differences between northern and southern Lake Edward inferred from AVHRR brightness temperatures for different dates in 1995 and 1996. Calculated as TNORTH – TSOUTH.

5.4 Lake Temperature Gradients by Remote Sensing

In the absence of specific calibration of calculated SSTs to Lake Edward, analyses were confined to assessment of temperature differences within the lake rather than to temperature in absolute terms. Temperature differences between north central Lake Edward and south central Lake Edward are plotted in Figure 4. Discernible and statistically significant temperature differences exist on most dates, but there is not a consistent gradient between north and south throughout the year. Instead, there is a tendency for the lake to be warmer in the south during the dry seasons and to be warmer in the north during rainy season conditions. Temperature differences of 1°C or greater are not uncommon.

6. DISCUSSION

Lake Edward has experienced striking variation in dissolved salt concentration during the last 35 years. These variations are partially climate related, based on the water balance model, and are consistent with the generally warmer, wetter conditions of the present high elevation tropics compared with conditions 40 years ago (Lehman, 1998). Chemical data are presented in Table 11 along a gradient of increasing conductivity and ionic strength, from measurements by Kilham (1972), Lehman *et al.* (1998), and Talling and Talling (1965). Ion activities were calculated from ionic strength by the Güntelberg approximation (Stumm and Morgan, 1970), using temperature coefficients at 25 °C (Stumm and Morgan, 1970, table 5.1), and ion activity products (IAP) were calculated. Chloride is used as a conservative reference solute for comparisons. Several points can be made that have implications for the sedimentary record of Lake Edward.:

1. Ca/Cl ratios decrease with evaporative concentration. Ca is differentially lost, probably as carbonate to the sediments.
2. Ca concentrations remain relatively constant, but Ca/Mg ratios fall with progressive salt concentration.
3. During the last 40 years Lake Edward has varied from being at the saturation point with respect to calcite, to being 18-fold supersaturated.

The pH and Ca/Mg ratios of Lake Edward indicate that dolomite should be the thermodynamically stable phase for the solid minerals (Stumm and Morgan, 1970, Figures 5-11), as is also true of sea water. In fact, as in sea water the precipitating mineral is mainly calcite, but the carbonate should have a variable composition of $MgCO_3$. The range of supersaturation reported in Table 11 is compatible with up to about 10% $MgCO_3$ in the carbonate solid phase (Stumm and Morgan, 1970, Figures 5-11); percentage composition should increase with conductivity and ionic strength of the lake water. Consequently, the observation of about 12% Mg content in the sedimentary calcite of Lake Edward is consistent with the high levels of supersaturation observed earlier in the 20th century rather than later. Ca/Mg ratios of

the precipitating carbonates may provide a proxy signal of changes in water balance through evaporative concentration and related changes. Sedimentary calcite is the result of (1) evaporative concentration of water already at the precipitation point, (2) elevated water temperature, or (3) increased rates of photosynthesis. Not all algal taxa can equally use bicarbonate as a carbon source (Prins and Elzenga, 1989; Riebesell *et al.*, 1993). Thus, the types of species that are stimulated under alternating conditions of water column stability or mixing may control some of the seasonality and isotopic composition of calcite deposition in Lake Edward.

Table 11. Chemical conditions affecting carbonate equilibria across a range of dilution states for Lake Edward. Ksp refers to calcite at 25 °C (Stumm & Morgan, 1970).

Analyst:	Kilham (1972)	Lehman *et al.* (1998)	Talling & Talling (1965)
Year	1969	1995	1961
Ionic Strength	0.007	0.012	0.015
Ca, μM	335	310	310
Ca/Cl	0.73	0.53	0.31
Ca/Mg	0.37	0.19	0.16
IAP/Ksp	0.95	10.2	17.9

Related arguments apply to the deposition of biogenic Si. Diatoms are not abundant at the surface sediments nor in the modern plankton. The dominant fossil diatom in the sediments of Lake Edward is *Cyclostephanos damasii*, a taxon formerly classified as *Stephanodiscus damasii* (Gasse *et al.*, 1983). This unicellular centric diatom has been identified as a low Si/P ratio species, with favorable stoichiometries near 1:1 by moles (Kilham *et al.*, 1986). Present day Lake Edward is very rich in SRSi (soluble reactive silicon), and the Si/P ratio is extremely high (ca. 200:1). These are not the typical conditions associated with success by *Cyclostephanos/Stephanodiscus*. Hence, its paucity in the plankton and the surface sediment is consistent with the chemistry, but the lake must have exhibited alternate states under perhaps altered climate conditions and mixing regimes that promoted vast production of these diatoms in the recent past.

One hypothesis for the paucity of diatoms in Lake Edward at present, particularly in the north, is that increased water column stability enhances diatom loss rates by sinking (E. Ralph, pers. comm.). The presumed mechanism would be a warmer surface layer resulting from the warm discharge of Lake George through the Kazinga channel during the rainy season. Water temperatures are in fact occasionally warmer in the north than in the south during the rainy months of April and May (Figure 4), but at other times the surface water is warmer in the south. The spatial pattern reported by Hecky and Kling (1987) was observed in samples collected in mid-March 1972, a month that can exhibit the start of rainy season conditions.

Sensitivity analyses which predict the responses of lake surface temperature and evaporation rates to climate changes also document predicted changes in lake mixing dynamics. Changes in wind speed, cloud cover, and other climate factors can

theoretically increase or diminish the period of deep mixing in Lake Edward by weeks or months. It is plausible that altered mixing regimes under alternate climate scenarios have been the cause of the great variations in diatom success within the lake, as recorded in its sediments.

The heat balance model for Lake Edward and existing meteorological data indicate that temporal variations in wind speed and radiation balance owing to cloud cover are the dominating sources of variation in both lake temperature and evaporation (Tables 5 and 6). Model simulations were based on independent perturbation of individual climate variables. Any empirical positive correlations between wind speed and either air temperature or irradiance would tend to subdue the predicted effects on lake temperature, but would exaggerate effects on evaporation. Irrespective of these secondary effects which may amplify the variations in evaporation rate, it is clear that Lake Edward has exhibited wide variations in water turnover and evaporative concentration of dissolved salts in this century alone.

The methods used to estimate temperature and evaporation for Lake Edward may have wide application to tropical lakes in general, and in particular to the great lakes of East Africa. Similarly, sensitivity analyses based on these solution methods, using empirical variations in input variables as reference, should permit quantitative prediction of lake response to specific climate change scenarios.

7. CONCLUSIONS AND RECOMMENDATIONS

Lake Edward resonates strongly to climate change signals. Its water detention time is relatively short compared with other great lakes of the region, but the unusual geochemical composition of its inputs from the south interact with water balance to produce striking changes in chemistry and ionic strength. The lake is of adequate size to be investigated with existing satellite technology, and it exhibits temporal and spatial patterns that appear to be correlated with climate. The data sets and models developed for this study successfully brought into focus issues that require further field work, remote sensing, and additional development of theory. These are:

1. Improved elevation maps are needed to corroborate or refine the existing DEM for the region, to define more precisely the total area of drainage, and to partition the relative areas of sub-catchments with differing stream chemistry.
2. Water samples must be collected seasonally from the Ruchuru River and other streams entering Lake Edward from the south. Chemical analyses of these waters should be used to test the *a priori* hypothesis of their composition and their potential for altering the water chemistry of Lake Edward.
3. The discharge flow of the Semliki River at its source must be measured in order to test the validity of predicted water balance (Table 4). Furthermore, measurements are needed for the discharge flow of the southern rivers.

4. Ca/Mg ratios of sedimentary carbonates should be investigated as an index of lake water balance.
5. More precise estimates of cloud cover and wind speed over Lake Edward are required, and any cloudiness differences between day and night should be quantified.
6. Additional AVHRR scenes of Lake Edward from multiple years should be assembled to test the generality of surface temperature differences between lake regions in different seasons. An effort should be made to assess the accuracy of the temperature estimates in absolute terms. Then the heat balance model for the lake can be tested using remotely sensed temperatures.

ACKNOWLEDGMENTS

This research was funded in part by grants from the National Geographic Society and the U. S. National Science Foundation. D. A. Lehman assembled and organized the data sets on which this study was based. T. Lærdal provided unpublished bathymetric maps of Lake Edward and made valuable comments on the content of the paper. J. Russell provided unpublished information about sediment composition and accumulation rates. D. Gesch provided information about the USGS digital elevation model and its derivative products.

REFERENCES

Bugenyi, F.W.B. (1982) Copper pollution studies in Lakes George and Edward, Uganda: The distribution of Cu, Cd and Fe in the water and sediments. *Environmental Pollution (Series B)* **3**, 129-138.

Burgis, M. J., Dunn, L. G., Ganf, G. G., McGowan, L. M., and Viner, A. B. (1972) Lake George, Uganda. Studies on a tropical freshwater ecosystem, in K. Kajak and A. Hillbricht-Ilkowska (eds.), *Productivity Problems in Freshwaters*, Polish Scientific Publications, Warszawa-Krakow, pp. 301-309.

Croley, T.E. (1989) Verifiable evaporation modeling on the Laurentian Great Lakes. *Water Resources Research* **25**, 781-792.

DCW (1993) *Digital Chart of the World 1993 version on-line*, Pennsylvania State University Libraries, www.maproom.psu.edu/dcw/.

Degens, E.T. (1973) Hydrothermal origin of metals in some East African rift lakes. *Mineralium Deposita* **8**, 388-404.

Gasse, F., Talling, J.F., and Kilham, P. (1983) Diatom assemblages in East Africa: classification, distribution and ecology. *Revue d'Hydrobiologie Tropicale* **16**, 3-34.

Hecky, R.E., and Kling, H.J. (1987) Phytoplankton ecology of the Great Lakes in the rift valleys of central Africa. *Archiv für Hydrobiologie Ergebisse Limnologie* **25**, 197-228.

Hurst, H.E. (1927) *The lake plateau basin of the Nile*. Egyptian Ministry of Public Works. Physical Department paper No. 23, 66 p.

Hydromet (1991) *Hydrometeorological survey of the catchments of Lakes Victoria, Kyoga and Albert. Summaries of meteorological data observed over the project area.* Hydromet Survey Project Report, Entebbe.

ILEC (2000) *Lake Edward*, World Lakes Database, International Lake Environment Committee Foundation. http://www.ilec.or.jp/

Imberger, J. and Patterson, J.C. (1990) Physical Limnology, in J.W. Hutchinson and T.Y. Wu (eds.), *Advances in Applied Mechanics* **27**, 303-475.

Johnson, T.C. and 8 others. (1996) Late Pleistocene desiccation of Lake Victoria and rapid evolution of cichlid fishes. *Science* **273**, 1091-1093.

Johnson, T.C. and Odada, E. (1996) *The limnology, climatology, and paleoclimatology of the East African lakes*, Gordon and Breach.

Johnson, T.C., Chan, Y., Beuning, K.R.M., Kelts, K., Ngobi, G., and Verschuren, D. (1998) Biogenic silica profiles in Holocene cores from Lake Victoria: Implications for lake level history and initiation of the Victoria Nile, in J. T. Lehman (ed.), *Environmental change and response in East African lakes*, Kluwer Academic Publishers, Dordrecht, pp. 75-88.

Kilham, P. (1972) *Biogeochemistry of African lakes and rivers*, Ph. D. thesis, Duke University, 197 p.

Kilham, P. and Hecky, R.E. (1973) Fluoride: geochemical and ecological significance in East African waters and sediments. *Limnology and Oceanography* **18**, 932-945.

Kilham, P. (1984) Sulfate in African inland waters: Sulfate to chloride ratios. *Verhandlungen der Internationale Vereinigung für Limnology* **22**, 296-302.

Kilham, P., Kilham, S.S., and Hecky, R.E. (1986) Hypothesized resource relationships among African planktonic diatoms. *Limnology and Oceanography* **31**, 1169-1181.

Keijman, J.Q. (1974) The estimation of the energy balance of a lake from simple weather data. *Boundary-Layer Meteorology* **7**, 399-407.

Lærdal, T., Talbot, M.R. and Russell, J. (2001) Late Quaternary Sedimentation and Climate in the Lakes Edward and George area, Uganda-Congo, in E. Odada and D. Olago (eds.), *The East African Great Lakes: Limnology, Paleolimnology, and Biodiversity*, Kluwer Academic Publishers, Dordrecht.

Lehman, J.T. (1998) The role of climate change in the modern condition of Lake Victoria. *Theoretical and Applied Climatology* **61**, 29-37.

Lehman, J.T., Litt, A.H., Mugidde, R., and Lehman, D.A. (1998) Nutrients and plankton biomass in the rift lake sources of the White Nile: Lakes Albert and Edward, in J.T. Lehman (ed.), *Environmental Change and Response in East African Lakes*, Kluwer Academic Publishers, Dordrecht, pp. 157-172.

Maidment, D.R. (editor) (1993) *Handbook of hydrology*, McGraw-Hill.

Monismith, S.G. (1985) Wind-forced motions in stratified lakes and their effect on mixed-layer shear. *Limnology and Oceanography* **30,** 771-783.

Niiler, P.P., and Kraus, E.B. (1977) One-dimensional models of the upper ocean, in E.B. Kraus (ed.), *Modelling and prediction of the upper layers of the ocean*, Pergamon, pp. 143-172.

Price, J.F. (1981) Upper ocean response to a hurricane. *Journal of Physical Oceanography* **11**, 153-175.

Prins, H.B.A. and Elzenga, J.T.M. (1989) Bicarbonate utilization: function and mechanism. *Aquatic Botany* **34**, 59-83.

Riebesell, U., Wolf-Gladrow, D. A. and Smetacek, V. (1993) Carbon dioxide limitation of marine phytoplankton growth rates. *Nature* **361**, 249-251.

Ruff, I. and A. Gruber, 1988: General Determination of Earth Surface Type and Cloud Amount Using Multispectral AVHRR Data. *NOAA Technical Report NESDIS 39*, U. S. Dept. Comm., NOAA, NESDIS, Washington, D. C. 30 p.

Sherman, F.S., Imberger, J., and Corcos, G.M. (1978) Turbulence and mixing in stably stratified waters. *Annual Review of Fluid Mechanics* **10**, 267-288.

Spigel, R.H. (1980) Coupling of internal wave motion with entrainment at the density interface of a two-layer lake. *Journal of Physical Oceanography* **10**, 144-155.

Spigel, R.H., and Imberger, J. (1980) The classification of mixed-layer dynamics in lakes of small to medium size. *Journal of Physical Oceanography* **10**, 1104-1121.

Spigel, R.H., Imberger, J., and Rayner, K.N. (1986) Modeling the diurnal mixed layer. *Limnology and Oceanography* **31**, 533-556.

Strub, P.T. and Powell, T.M. (1987) The exchange coefficients for latent heat and sensible heat flux over lakes: dependence upon atmospheric stability. *Boundary-Layer Meteorology* **40**, 349-361.

Stumm, W. and Morgan, J. (1970) *Aquatic Chemistry*, Wiley.

Talbot, M. R., Williams, M. A. J. and Adamson, D. A. (2000) Strontium isotope evidence for late Pleistocene reestablishment of an integrated Nile drainage network. *Geology* **28**, 343-346.

Talling, J. F. and Talling, I. B. (1965) The chemical composition of African lake waters. *Internationale Revue gesamten Hydrobiologie* **50**, 421-463.

Viner, A. B. (1969) The chemistry of the water of Lake George, Uganda. *Verhandlungen der Internationale Vereinigung für Limnology* **17**, 289-296.

Viner, A.B. and Smith, I.R. (1973) Geographical, historical and physical aspects of Lake George. *Proceedings of the Royal Society of London, Series B* **184**, 235-270.

Visser, S. (1961) Chemical composition of rain water in Kampala, Uganda, and its relation to meteorological and topographical conditions. *Journal of Geophysical Research* **66**, 3759-3765.

Visser, S.A. (1974) Composition of waters of lakes and rivers in East and West Africa. *African Journal of Tropical Hydrobiology and Fisheries* **3**, 43-59.

Worthington, E.B. (1932) *A report on the fisheries of Uganda investigated by the Cambridge Expedition to the East African lakes, 1930-31. Part 1. Lakes Edward and George and the Kazinga Channel*, Zoological Laboratory, Cambridge, June 1932.

Yin, X. and Nicholson, S.E. (1998) The water balance of Lake Victoria. *Hydrological Sciences Journal* **43**, 789-811.